PROCEEDINGS OF SCIENCE

Recent results from the SND detector

V. P. Druzhinin*[ab], M. N. Achasov[ab], A. Yu. Barnyakov[ab], K. I. Beloborodov[ab], A. V. Berdyugin[ab], A. G. Bogdanchikov[a], A. A. Botov[a], T. V. Dimova[ab], V. B. Golubev[ab], L. V. Kardapoltsev[ab], A. G. Kharlamov[ab], A. A. Korol[ab], S. V. Koshuba[a], D. P. Kovrizhin[ab], A. S. Kupich[a], K. A. Martin[a], A. E. Obrazovsky[a], E. V. Pakhtusova[a], S. I. Serednyakov[ab], D. A. Shtol[ab], Z. K. Silagadze[ab], I. K. Surin[ab], Yu. V. Usov[ab] and A. V. Vasiljev[ab].

[a] *Budker Institute of Nuclear Physics, Novosibirsk, 630090, Russia*
[b] *Novosibirsk State University, Novosibirsk, 630090, Russia*
E-mail: druzhinin@inp.nsk.su

Recent results on study of exclusive processes of e^+e^- annihilation into hadrons below 2 GeV obtained at the SND detector are presented. The analyses are based on data collected at the VEPP-2M and VEPP-2000 colliders. In particular, we present the precise measurements of the $e^+e^- \to \pi^0\gamma$ and $e^+e^- \to K^+K^-$ cross sections, and the first measurements of the $e^+e^- \to \omega\pi^0\eta$ and $e^+e^- \to \pi^+\pi^-\pi^0\eta$ reactions.

The European Physical Society Conference on High Energy Physics
5-12 July, 2017
Venice

*Speaker.

PoS(EPS-HEP2017)371

Table 1: The distribution of integrated luminosity (IL) recorded by SND at VEPP-2M and VEPP-2000 over different energy regions. At VEPP-2M the minimum and maximum energies are 0.36 and 1.4 GeV.

Energy range (GeV)	0.30 – 0.97	0.98 – 1.06	1.06 – 2.00
IL at VEPP-2M (pb^{-1})	9.1	13.2	8.8
IL at VEPP-2000 (pb^{-1})	15.4	6.9	~ 100

1. Introduction

SND [1, 2, 3, 4] is the universal nonmagnetic detector consisting of a nine-layer drift chamber, aerogel Cherenkov counters, a three-layer spherical electromagnetic calorimeter with 1640 NaI(Tl) crystals, and a muon system.

SND collected data at two e^+e^- colliders: VEPP-2M [5] during 1996-2000 in the center-of-mass energy range 0.36-1.38 GeV and VEPP-2000 [6] starting from 2010 in the energy range 0.3-2.0 GeV. During the 2010-2013 data taking period the luminosity was limited by the deficit of positrons. From 2014 the VEPP-2000 accelerator complex was under reconstruction. The experiments were restarted by the end of 2016 with a new 10 times more intensive positron source. The data sample with an integrated luminosity of about 60 pb^{-1} has been collected during 2017. The achieved luminosity near 2 GeV is about 4×10^{31} cm^{-2}s^{-1}. The distributions of integrated luminosities recorded at VEPP-2M and VEPP-2000 over different energy regions are presented in Table 1.

Main physics task of the SND experiment is study of all possible processes of e^+e^- annihilation into hadrons below 2 GeV. In particular, these measurements are used to obtain the total hadronic cross section needed for Standard Model calculation of the anomalous magnetic moment of muon and running electromagnetic coupling constant. A detailed study of dynamic of exclusive processes is also performed. In this report we present SND results on four processes: $e^+e^- \to \pi^0\gamma$, $e^+e^- \to K^+K^-$, $e^+e^- \to \omega\pi^0\eta$ and $e^+e^- \to \pi^+\pi^-\pi^0\eta$.

2. Precise measurements of the $e^+e^- \to \pi^0\gamma$ and $e^+e^- \to K^+K^-$ cross sections

The $e^+e^- \to \pi^0\gamma$ cross section is the third largest cross section (after $e^+e^- \to \pi^+\pi^-$ and $\pi^+\pi^-\pi^0$) below 1 GeV. From analysis of the $e^+e^- \to \pi^0\gamma$ data in the vector meson dominance (VMD) model, the widths of vector-meson radiative decays are extracted, which are widely used in phenomenological models. The most accurate data on this process were obtained in experiments at the VEPP-2M e^+e^- collider with the SND [7, 8] and CMD-2 [9] detectors. The SND results [7, 8] are based on about 25% of data collected at VEPP-2M. Here we present a new analysis [10] using the full SND@VEPP-2M data sample.

The new SND data on the $e^+e^- \to \pi^0\gamma$ cross section shown in Fig. 1 in five energy regions agree with previous measurements within the systematic uncertainties, but are significantly more precise. From the fit to cross section data we obtain the products of branching fractions:

$$\begin{aligned} B(\rho \to \pi^0\gamma)B(\rho \to e^+e^-) &= (1.98 \pm 0.22 \pm 0.10) \times 10^{-8}, \\ B(\omega \to \pi^0\gamma)B(\omega \to e^+e^-) &= (6.336 \pm 0.056 \pm 0.089) \times 10^{-6}, \\ B(\phi \to \pi^0\gamma)B(\phi \to e^+e^-) &= (4.04 \pm 0.09 \pm 0.19) \times 10^{-7}. \end{aligned} \tag{2.1}$$

PoS(EPS-HEP2017)371

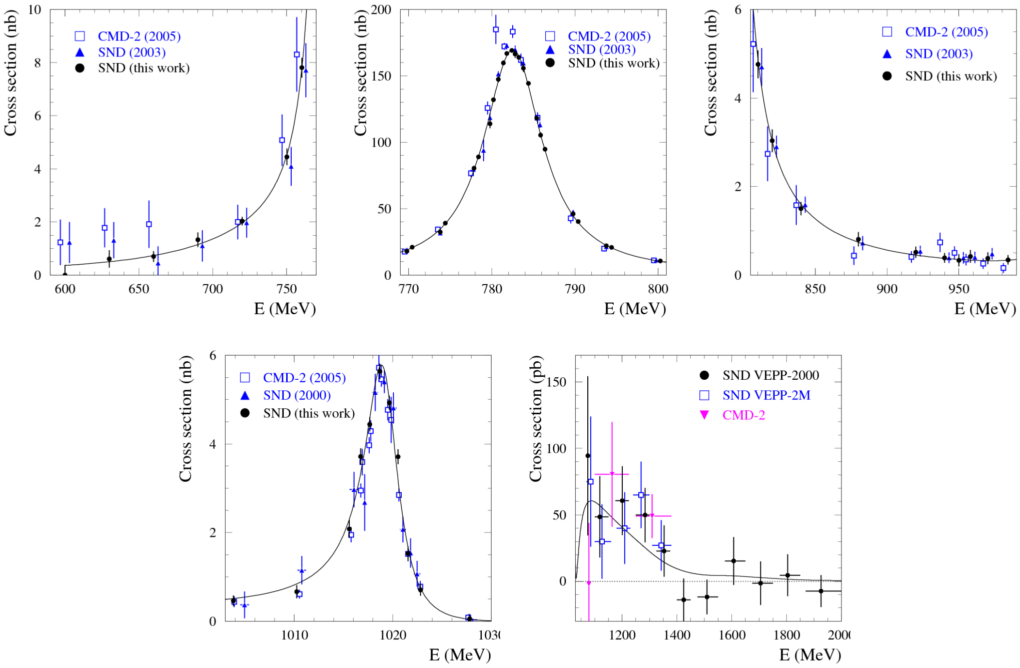

Figure 1: The $e^+e^- \to \pi^0\gamma$ cross section measured by SND using the full VEPP-2M data sample in comparison with the previous most accurate measurements. The curve is the result of the VMD fit. Only statistical errors are shown. The systematic errors are 3.2%, 3%, and 6% for SND (2000), SND (2003), and CMD-2 (2005) data, respectively. The systematic uncertainty of the current measurement at the ω and ϕ peaks is 1.4%. In the highest energy region the preliminary SND result based on VEPP2000 data is shown.

In highest energy region in Fig. 1, the preliminary result based on VEPP-2000 data collected in 2010-2013 with an integrated luminosity of 37 pb^{-1} are shown. At energies below 1.4 GeV the cross-section data obtained at VEPP-2000 agrees with VEPP-2M measurements. In the energy range 1.1-1.4 GeV we see the contribution of the $\omega(1420)$ and $\rho(1450)$ resonances. The cross section in the energy region 1.4–2.0 GeV is small indicating that that the probabilities of the decays to $\pi^0\gamma$ of $\omega(1680)$ and $\rho(1700)$ are small.

We also improve accuracy of $e^+e^- \to K^+K^-$ cross section measurement in the energy range 1.05–2.00 GeV. Figure 2 represents the SND measurement of the $e^+e^- \to K^+K^-$ cross section [11] in comparison with the most precise previous measurement by BABAR [12].

3. Previously unmeasured cross sections

The process $e^+e^- \to \omega\pi^0\eta$ is studied in the seven-photon final state [13]. The measured $e^+e^- \to \omega\pi^0\eta$ cross section is shown in Fig. 3 (left). Figure 3 (right) shows the $\pi^0\eta$ mass distribution for selected $\omega\pi^0\eta$ events, which is well described by the model of the $\omega a_0(980)$ intermediate state.

The process $e^+e^- \to \pi^+\pi^-\pi^0\eta$ has complex internal structure. Our preliminary study show that there are at least four mechanisms for this reaction: $\omega\eta$, $\phi\eta$, $a_0(980)\rho$, and structureless $\pi^+\pi^-\pi^0\eta$. The known $\omega\eta$ and $\phi\eta$ contributions explain about 50-60% of the cross section be-

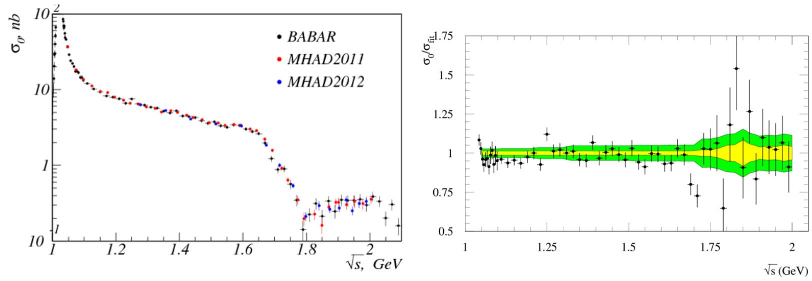

Figure 2: Left panel: The $e^+e^- \to K^+K^-$ cross section measured by SND at VEPP2000 and in the BABAR experiment. Right panel: The relative difference between the $e^+e^- \to K^+K^-$ cross sections measured by BABAR and the fit to the SND data. The SND and BABAR systematic uncertainties are shown by the light and dark shaded bands, respectively.

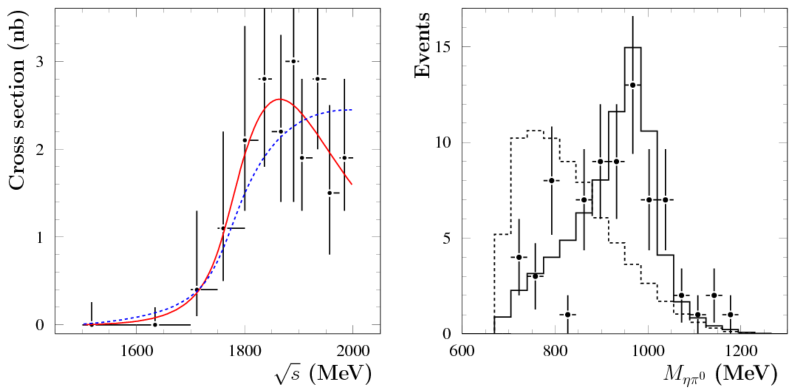

Figure 3: Left panel: The $e^+e^- \to \omega\eta\pi^0$ cross section measured by SND. The solid (dashed) curve shows the result of the fit in the model of $\omega a_0(980)$ intermediate state with (without) a resonance contribution. Right panel: The $\eta\pi^0$ invariant mass spectrum for selected $e^+e^- \to \omega\eta\pi^0$ events. The solid histogram represents $e^+e^- \to \omega a_0(980)$ simulation, while the dashed histogram represents $\omega\eta\pi^0$ phase-space simulation.

low 1.8 GeV. Above 1.8 GeV the dominant mechanism is $a_0\rho$. The preliminary result on the $e^+e^- \to \pi^+\pi^-\pi^0\eta$ cross section is shown in Fig. 4 (left). The cross section for the subprocess $e^+e^- \to \omega\eta$ is measured separately [14] and shown in Fig. 4 (right) in comparison with the BABAR measurement [15]. Our results have better accuracy and disagree with the BABAR data at $E > 1.6$ GeV. Both the previously unmeasured cross sections discussed in this section give a sizable contribution ($\sim 5\%$) to the total hadronic cross section.

Acknowledgments

This work is supported in part by the RFBR grants 16-02-00327 and 16-02-00014. Part of this work related to the photon reconstruction algorithm in the electromagnetic calorimeter is supported by the Russian Science Foundation (project No. 14-50-00080).

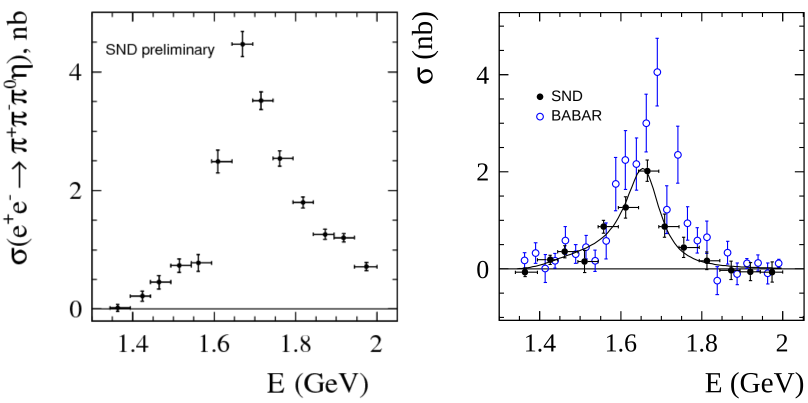

Figure 4: Left panel: The $e^+e^- \to \pi^+\pi^-\pi^0\eta$ cross section measured by SND. Right panel: The $e^+e^- \to \omega\eta$ cross section measured by SND in comparison with BABAR data [15]. The curve is the result of the VMD fit.

References

[1] M. N. Achasov *et al.*, Nucl. Instrum. Methods Phys. Res., Sect. A **598**, 31 (2009).

[2] V. M. Aulchenko *et al.*, Nucl. Instrum. Methods Phys. Res., Sect. A **598**, 102 (2009).

[3] A. Y. Barnyakov *et al.*, JINST **9**, C09023 (2014).

[4] V. M. Aulchenko *et al.*, Nucl. Instrum. Methods Phys. Res., Sect. A **598**, 340 (2009).

[5] I. A. Koop *et al.*, in *Proceedings of the Workshop on Physics and Detectors for DAPHNE*, Frascati, Italy, 1999 (Frascati, 1999), p. 393.

[6] A. Romanov *et al.*, in *Proceedings of Particle Accelerator Conference PAC 2013, Pasadena, CA USA, 2013*, p. 14.

[7] M. N. Achasov *et al.* (SND Collaboration), Eur. Phys. J. C **12**, 25 (2000).

[8] M. N. Achasov *et al.* (SND Collaboration), Phys. Lett. B **559**, 171 (2003).

[9] R. R. Akhmetshin *et al.* (CMD-2 Collaboration), Phys. Lett. B **605**, 26 (2005).

[10] M. N. Achasov *et al.* (SND Collaboration), Phys. Rev. D **93**, 092001 (2016).

[11] M. N. Achasov *et al.* (SND Collaboration), Phys. Rev. D **94**, 112006 (2016).

[12] J. P. Lees *et al.* (BaBar Collaboration), Phys. Rev. D **88**, 032013 (2013).

[13] M. N. Achasov *et al.* (SND Collaboration), Phys. Rev. D **94**, 032010 (2016).

[14] M. N. Achasov *et al.* (SND Collaboration), Phys. Rev. D **94**, 092002 (2016).

[15] B. Aubert *et al.* (BABAR Collaboration), Phys. Rev. D **73**, 052003 (2006).

PoS(EPS-HEP2017)371